



## Stress-strain state during the formation of normal cracks in three-layer bendable reinforced concrete elements under the action of longitudinal and transverse forces

Korol O.A.<sup>1</sup> , Barabanova T.A.<sup>1</sup> \*, Sabitov L.S.<sup>3</sup> ,  
Abdullazyanov E.U.<sup>2</sup> , Ayzatullin M.M.<sup>2</sup> 

<sup>1</sup> National Research Moscow State University of Civil Engineering, Moscow, Russia,

<sup>2</sup> Kazan State Energy University, Kazan, Russia,

<sup>3</sup> Kazan (Volga Region) Federal University, Kazan, Russia

**Abstract.** Most wall panels in operating multi-storey residential buildings are in a complex stress-strain state under the influence of vertical and horizontal loads, such as their own weight, wind, etc. These features must be taken into account in the calculation in order to ensure operational safety. The combination of vertical and horizontal forces acting simultaneously for three-layer bending elements leads to the fact that the boundary between the compressed and tensile zones not only moves from one layer to another, but also has a different geometric shape depending on the ratio between the vertical and horizontal load. The stress-strain state during the formation of normal cracks in three-layer bendable reinforced concrete elements is caused by the impact on layers of different concretes. The formation of normal cracks occurs due to the achievement of ultimate tensile strength by the most stretched concrete under the influence of external loads. Since three-layer reinforced concrete elements consist of two outer layers (reinforced concrete) and a middle layer (lightweight concrete), when such an element bends, the outer layers are subject to compression, and the middle layer is subject to tension. The boundary of the compressed zone can be located either in one of the outer layers or intersect the middle layer, which falls into both the compressed and stretched zones. To analyze the stress-strain state during the formation of normal cracks, it is necessary to take into account the following parameters: geometric characteristics of the element (dimensions and shape of the section, layer thickness, etc.), physical and mechanical properties of concrete (compressive and tensile strength, elastic modulus, Poisson's ratio, crack resistance coefficient, etc.), characteristics of reinforcement (class, diameter, pitch of bars, etc.) and its location in the section.

**Keywords:** calculation algorithm for crack formation, three-layer enclosing structures, curtain wall panels, bending of structures

**Please cite this article as:** Korol O.A., Barabanova T.A., Abdullazyanov E.U., Sabitov L.S., Ayzatullin M.M. Stress-strain state during the formation of normal cracks in three-layer bendable reinforced concrete elements under the action of longitudinal and transverse forces. *Construction Materials and Products*. 2024. 7 (1). 3. DOI: 10.58224/2618-7183-2024-7-1-3

\*Corresponding author E-mail: [BarabanovaTA@mgsu.ru](mailto:BarabanovaTA@mgsu.ru).

## 1. INTRODUCTION

The main starting points for the calculation of the formation of cracks in bendable three-layer reinforced concrete elements with outer layers of structural concrete and a middle layer of low-strength concrete are considered by the authors of a number of works [1-6]. Most of them, when constructing calculation models, take into account the effect of only one prevailing force influence, neglecting the rest, less significant ones. For example, for curtain wall panels - these are horizontal wind loads [7-10], load-bearing walls - their own weight and the weight of overlying structures, floor panels and coatings - their own weight and technological or climatic influences. If the section of a multilayer structure experiences both vertical and horizontal impacts, the accuracy of the calculation is determined by modeling various possible cases of the position of the neutral line.

When constructing a calculation algorithm for the formation of cracks during bending of multilayer structures with monolithically connected concrete layers of different strengths, the authors of the theoretical and experimental studies used and verified the basic principles for calculating reinforced concrete elements under plane bending:

- sections remain flat after deformation;
- the greatest relative elongation of the outermost compressed fiber of concrete is equal to  $2R_{bt,ser}/E_b$ ;
- stresses in the concrete of the compressed zone are determined taking into account the elastic deformations of the concrete;
- stresses in the concrete of the tensile zone are distributed evenly and are equal  $R_{bt,ser}$

When constructing the calculated dependencies, the difference in the strength and deformation characteristics of the outer layers made of structural concrete and the inner layer made of low-strength concrete is taken into account, as well as the presence of normal tensile forces caused by concrete shrinkage [11-16]. The location of the reinforcement bars in the section of the element is assumed to be discrete.

## 2. METHODS AND MATERIALS

When constructing a calculation algorithm for the formation of cracks during bending of structures caused by the simultaneous action of horizontal and vertical forces, the basic principles for calculating reinforced concrete elements under plane bending were used.

The resultant of compressive forces in concrete can be represented by a certain integral of the distribution function of normal compressive stresses over the area of the compressed zone of concrete:

$$N_b = \iint_{AB} \sigma(x, y) dx dy \quad (1)$$

at voltage value

$$\sigma_b(x, y) = \frac{\sigma_b \sin \gamma}{x} \left( \frac{x}{\sin \gamma} - \frac{x \cos \gamma}{\sin \gamma} - y \right), \quad (2)$$

where  $\sigma_b$  is the maximum stress in the outermost compressed fiber of concrete;

$x$  – height of the compressed zone of concrete;

$\gamma$  is the angle of inclination of the plane of action of the moment of external forces to the vertical.

Depending on the angle of inclination of the force plane to the vertical, eight cases of the position of the neutral line in the section of the element are possible. Various cases of the position of the neutral line and the stress-strain state adopted in the calculation for the formation of cracks are shown in Fig. 1.

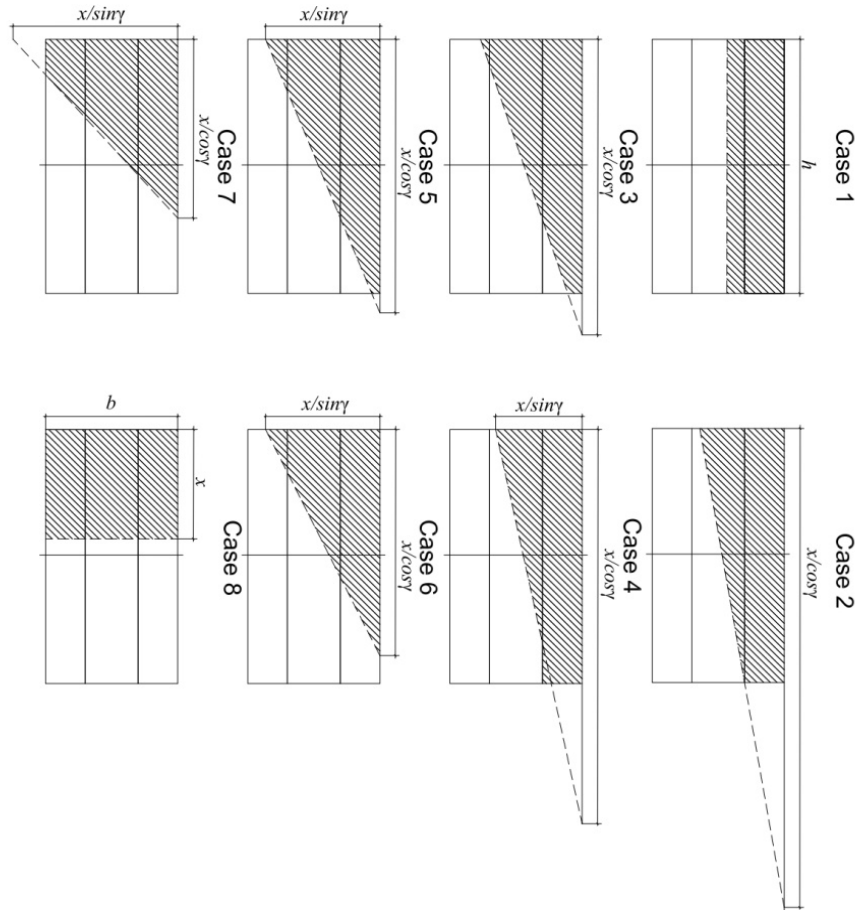


**Fig. 1.** Various cases of the position of the neutral line when calculating the formation of cracks under the action of horizontal and vertical loads.

Let's consider the derivation of calculation formulas for the compressed zone of concrete in the trapezoid formula (Fig. 1, case 2).

$$\begin{aligned}
 N_b &= \iint_{AB} \sigma(x, y) dx dy = \iint_{AB} \frac{\sigma_b \sin \gamma}{x} \left( \frac{x}{\sin \gamma} - \frac{x \cos \gamma}{\sin \gamma} - y \right) dx dy = \\
 &= \frac{\sigma_b \sin \gamma}{x} \int_0^{b_1} dy \int \left( \frac{x}{\sin \gamma} - \frac{x \cos \gamma}{\sin \gamma} - y \right) dx \\
 &+ n \int_{b_1}^{(b_1+b_2)} dy \int_0^{\left(\frac{x}{\cos \gamma} - y \operatorname{tg} \gamma\right)} \left( \frac{x}{\sin \gamma} - \frac{x \cos \gamma}{\sin \gamma} - y \right) dx + \int_{(b_1+b_2)}^b dy \int_0^{\left(\frac{x}{\cos \gamma} - y \operatorname{tg} \gamma\right)} \left( \frac{x}{\sin \gamma} - \frac{x \cos \gamma}{\sin \gamma} - y \right) dx = \frac{\sigma_b \sin \gamma}{x} \\
 &\times \times \left[ \left( \frac{y^3}{6} \operatorname{tg} \gamma + \frac{yx^2}{2 \sin \gamma \cos \gamma} - \frac{y^2 x}{2 \cos \gamma} \right) \Big|_0^{b_1} + n \left( \frac{x^2 y}{\sin 2\gamma} + \frac{y^3}{6} \operatorname{tg} \gamma - \frac{y^2 x}{2 \cos \gamma} \right) \Big|_{b_1}^{(b_1+b_2)} \right. \\
 &\left. + \left( \frac{yx^2}{\sin 2\gamma} + \frac{y^3}{6} \operatorname{tg} \gamma - \frac{y^2 x}{2 \cos \gamma} \right) \Big|_{(b_1+b_2)}^b \right] = \\
 &= \frac{\sigma_b \sin \gamma}{x} \left\{ \frac{x^2 b_1}{\sin 2\gamma} + \frac{b_1^3}{6} \operatorname{tg} \gamma - \frac{b_1^2 x}{2 \cos \gamma} + n \left[ \frac{x^2 b_2}{\sin 2\gamma} + \frac{c}{6} \operatorname{tg} \gamma + \frac{x K_2}{2 \cos \gamma} \right] + \frac{x^2 b_3}{\sin 2\gamma} + \frac{c}{6} \operatorname{tg} \gamma - \frac{x K_2}{2 \cos \gamma} \right\} \\
 &= \frac{\sigma_b \operatorname{tg} \gamma}{2x} \left\{ n \left[ \frac{x^2 b_3}{\sin \gamma} + \frac{\sin \gamma}{3} c - x K_2 \right] + \frac{x^2 (b_1 + b_3)}{\sin \gamma} + \frac{\sin \gamma}{3} c + x K_2 \right\} \\
 &= \frac{\sigma_b \operatorname{tg} \gamma}{2x} \left[ \frac{x^2 b_n}{\sin \gamma} + \frac{\sin \gamma}{3} c (n + 1) - x K_2 (n + 1) \right], \quad (3)
 \end{aligned}$$

where  $b_n = b_1 + nb_2 + b_3$  – total width of the element section;

$n = E_{b2}/E_{b1}$  – the ratio of the initial elastic modulus of the middle thermal insulation layer to the initial elastic modulus of the outer layers.

The stress of the most compressed concrete fiber in accordance with those accepted in Fig.1. notation equals:

$$\sigma_b = \varepsilon_b E_b = \varepsilon_{ut} \frac{x}{H \cdot x} \cdot E_b = \frac{2R_{bt,ser}}{E_b} \cdot \frac{x E_b}{H \cdot x} = \frac{2R_{bt,ser} \cdot x}{b \sin \gamma + h \cos \gamma - x} \quad (4)$$

After substituting (4) into (3), we obtain the final formula for determining the resultant compressive forces in concrete:

$$\begin{aligned} N_b &= \frac{R_{bt,ser1} t g \gamma}{b \sin \gamma + h \cos \gamma - x} \left\{ n \left[ x^2 b_2 - \frac{\sin \gamma}{3} [(b_1 + b_2)^3 - b_1^3] - x[(b_1 + b_2)^2 - b_1^2] \right. \right. \\ &\quad \left. \left. + \frac{x^2 (b_1 + b_2)}{\sin \gamma} + \frac{\sin \gamma}{3} [b^3 - (b_1 + b_2)^3 + b_1^3] - x[b^2 - (b_1 + b_2)^2 + b_1^2] \right] \right\} \\ &= \frac{R_{bt,ser1} t g \gamma}{b \sin \gamma + h \cos \gamma - x} \cdot \left[ \frac{x^2 b_n}{\sin \gamma} + \frac{\sin \gamma}{3} (n K_3 + K_4) - x(n K_1 + K_2) \right], \end{aligned} \quad (5)$$

where

$$\begin{aligned} K_1 &= (b_1 + b_2)^2 - b_1^2; \\ K_2 &= b^2 - (b_1 + b_2)^2 + b_1^2; \\ K_3 &= (b_1 + b_2)^3 - b_1^3; \\ K_4 &= b^3 - (b_1 + b_2)^3 - b_1^3, \end{aligned}$$

where  $R_{bt,ser1}$  – tensile strength of concrete outer layers.

Resultant of tensile forces in concrete:

$$\begin{aligned} N_{bt} &= \iint_{AB} R_{bt,ser1} dx dy - \int_0^{b_1} dy \int_{\left(\frac{x}{\cos \gamma} - y t g \gamma\right)}^h R_{bt,ser1} dx + \int_{b_1}^{(b_1+b_2)} dy \cdot \\ &\quad \int_{\left(\frac{x}{\cos \gamma} - y t g \gamma\right)}^h R_{bt,ser2} dx + \int_{(b_1+b_2)}^b dy \int_{\left(\frac{x}{\cos \gamma} - y t g \gamma\right)}^h R_{bt,ser1} dx = R_{bt,ser1} \left( h y - \frac{x y}{\cos \gamma} + \frac{y^2}{2} t g \gamma \right) \Big|_0^{b_1} \cdot \\ &\quad \int_{(b_1+b_2)}^b dy \int_{\left(\frac{x}{\cos \gamma} - y t g \gamma\right)}^h R_{bt,ser1} dx + R_{bt,ser2} \left( h y - \frac{x y}{\cos \gamma} + \frac{y^2}{2} t g \gamma \right) \Big|_{b_1}^{(b_1+b_2)} = R_{bt,ser1} \left( b_1 h - \right. \\ &\quad \left. \frac{x b_1}{\cos \gamma} + \frac{b_1^2}{2} t g \gamma + b_3 h - \frac{x b_3}{\cos \gamma} + \frac{A}{2} t g \gamma \right) + R_{bt,ser2} \left( b_2 h - \frac{x b_2}{\cos \gamma} + \frac{A}{2} t g \gamma \right) = R_{bt,ser1} \left[ b_m \left( h - \frac{x}{\cos \gamma} \right) + \right. \\ &\quad \left. \frac{(mA+B)}{2} t g \gamma \right], \end{aligned} \quad (6)$$

where  $m = R_{bt,ser2}/R_{bt,ser1}$ ;  $b_m = b_1 + m b_2 + b_3$ .

Static moment of the compressed part of the section relative to the x-axis:

$$\begin{aligned} S_x &= \iint_{AB} \sigma_b(x, y) y dx dy = \iint_{AB} \frac{\sigma_b \sin \gamma}{X} \left( \frac{X}{\sin \gamma} - \frac{x \cos \gamma}{\sin \gamma} - y \right) y dx dy = \\ &= \frac{\sigma_b \sin \gamma}{X} \int_0^{b_1} y dy \end{aligned}$$

$$\begin{aligned}
 & \cdot \int_0^{\frac{x}{\cos \gamma} - y \operatorname{tg} \gamma} \left( \frac{X}{\sin \gamma} - \frac{x \cos \gamma}{\sin \gamma} - y \right) dx + \int_{b_1}^{b_1+b_2} y dy \int_0^{\frac{x}{\cos \gamma} - y \operatorname{tg} \gamma} \left( \frac{X}{\sin \gamma} - \frac{x \cos \gamma}{\sin \gamma} - y \right) dx \\
 & + \int_{b_1}^{b_1+b_2} y dy \int_0^{\frac{x}{\cos \gamma} - y \operatorname{tg} \gamma} \left( \frac{X}{\sin \gamma} - \frac{x \cos \gamma}{\sin \gamma} - y \right) dx \Bigg] = \\
 & = \frac{\sigma_b \sin \gamma}{X} \left[ \left( \frac{X^2 y^2}{2 \sin 2\gamma} - \frac{X y^3}{3 \sin \gamma \cos \gamma} + \frac{y^4}{8} \tan \gamma \right) + \left( \frac{X^2 y^2}{2 \sin 2\gamma} - \frac{X y^3}{3 \cos \gamma} + \frac{y^4}{8} \tan \gamma \right) \right. \\
 & \quad \left. + \left( \frac{X^2 y^2}{2 \sin 2\gamma} + \frac{y^4}{8} \tan \gamma - \frac{X y^3}{3 \sin \gamma \cos \gamma} \right) \right] = \\
 & = \frac{\sigma_b \sin \gamma}{X} \left[ \frac{X^2 (nA+B)}{4 \sin \gamma} - \frac{X}{3} (nC + D) + (nE + F) \frac{\sin \gamma}{8} \right]
 \end{aligned} \tag{7}$$

where  $E = (b_1 + b_2)^4 - b_1^4$ ,  $F = b^4 - (b_1 + b_2)^4 + b_1^4$ .

Static moment of the compressed part of the section relative to the y-axis:

$$\begin{aligned}
 S_y & = \iint_{AB} \sigma_b(x, y) x dx dy = \iint \frac{\sigma_b \sin \gamma}{x} \left( \frac{x}{\sin \gamma} - \frac{x \cos \gamma}{\sin \gamma} - y \right) x dx dy \\
 & = \left[ \int_0^{b_1} dy \int_0^{\left(\frac{x}{\cos \gamma} - y \operatorname{tg} \gamma\right)} \left( \frac{x}{\sin \gamma} - \frac{x \cos \gamma}{\sin \gamma} - y \right) x dx \right. \\
 & \quad + n \int_{b_1}^{(b_1+b_2)} dy \int_0^{\left(\frac{x}{\cos \gamma} - y \operatorname{tg} \gamma\right)} \left( \frac{x}{\sin \gamma} - \frac{x \cos \gamma}{\sin \gamma} - y \right) x dx \\
 & \quad \left. + \int_{(b_1+b_2)}^b dy \cdot \int_0^{\left(\frac{x}{\cos \gamma} - y \operatorname{tg} \gamma\right)} \left( \frac{x}{\sin \gamma} - \frac{x \cos \gamma}{\sin \gamma} - y \right) x dx \right] \frac{\sigma_b \sin \gamma}{x} \\
 & = \frac{\sigma_b \sin \gamma}{x} \\
 & \cdot \left\{ n \left[ \frac{x^3 b_2}{6 \sin \gamma \cos^2 \gamma} + \frac{x K_4 \sin \gamma}{6 \cos^2 \gamma} - \frac{K_5}{24} \operatorname{tg}^2 \gamma - \frac{x^2 K_1}{4 \cos^2 \gamma} \right] + \frac{x^3 (b_1 + b_2)}{6 \sin \gamma \cos^2 \gamma} + \frac{x K_3 \sin \gamma}{6 \cos^2 \gamma} \right. \\
 & \quad \left. - \frac{K_6 \operatorname{tg}^2 \gamma}{24} - \frac{x^2 K_2}{4 \cos^2 \gamma} \right\} \frac{\sigma_b \sin \gamma}{x} \\
 & = \frac{\sigma_b \sin \gamma}{2x \cos^2 \gamma} \left[ \frac{x^3 b_n}{3 \sin \gamma} + \frac{x}{3} \sin \gamma \cdot (nK_3 + K_4) - \frac{x^2}{2} (nK_1 + K_2) \right. \\
 & \quad \left. - \frac{\sin^2 \gamma}{12} (nK_5 + K_6) \right].
 \end{aligned} \tag{8}$$

Static moment of the section of the tensioned part relative to the x-axis:

$$\begin{aligned}
 S_{xt} &= \iint_{AB} R_{bt,ser} y dx dy \\
 &= \int_0^{b_1} y dy \int_{\left(\frac{x}{\cos \gamma} - ytg\gamma\right)}^h R_{bt,ser1} dx \\
 &+ \int_{b_1}^{(b_1+b_2)} y dy \int_{\left(\frac{x}{\cos \gamma} - ytg\gamma\right)}^h R_{bt,ser1} dx \\
 &+ \int_{(b_1+b_2)}^{b_1} y dy \int_{\left(\frac{x}{\cos \gamma} - ytg\gamma\right)}^h R_{bt,ser1} dx \\
 &= R_{bt,ser1} \left[ \int_0^{b_1} \left( h - \frac{x}{\cos \gamma} + ytg\gamma \right) y dy \right. \\
 &+ m \int_{b_1}^{(b_1+b_2)} \left( h - \frac{x}{\cos \gamma} + ytg\gamma \right) y dy + \left. \int_{(b_1+b_2)}^b y \left( h - \frac{x}{\cos \gamma} + ytg\gamma \right) dy \right] \\
 &= R_{bt,ser1} \left[ \left( \frac{hy^2}{2} - \frac{y^2x}{\cos \gamma} + y^3tg\gamma \right) \right]_0^{b_1} \\
 &+ m \left( \frac{y^2h}{2} - \frac{y^2x}{\cos \gamma} + y^3tg\gamma \right) \Big|_{b_1}^{(b_1+b_2)} + \left( \frac{h}{2}y^2 - \frac{x}{\cos \gamma}y^2 + y^3tg\gamma \right) \Big|_{(b_1+b_2)}^b \\
 &= R_{bt,ser1} \left[ \frac{hK_2}{2} - \frac{xK_2}{2\cos \gamma} + \frac{b^3\sin^3\gamma}{3\cos \gamma} K_3 + m \left( \frac{hK_1}{2} - \frac{xK_1}{2\cos \gamma} + \frac{tg\gamma}{3} K_3 \right) \right] \\
 &= R_{bt,ser1} \left[ \left( h - \frac{x}{\cos \gamma} \right) \frac{(mK_1 + K_2)}{2} + \frac{tg\gamma}{3} (mK_3 + K_4) \right].
 \end{aligned} \tag{9}$$

Static moment of the section of the tensioned part relative to the y-axis:

$$\begin{aligned}
 S_{yt} &= \iint_{AB} R_{bt,ser} dy dx \\
 &= R_{bt,ser1} \left[ \int_0^{b_1} dy \int_{\left(\frac{x}{\cos \gamma} - ytg\gamma\right)}^h x dx \right. \\
 &+ m \int_{b_1}^{(b_1+b_2)} dy \cdot \int_{\left(\frac{x}{\cos \gamma} - ytg\gamma\right)}^h x dx + \left. \int_{(b_1+b_2)}^b dy \int_{\left(\frac{x}{\cos \gamma} - ytg\gamma\right)}^h x dx \right] \\
 &= R_{bt,ser1} \left[ \int_0^{b_1} \left( \frac{h^2}{2} - \frac{x}{2\cos^2\gamma} + \frac{xy\sin\gamma}{\cos^2\gamma} - \frac{y^2}{2}tg^2\gamma \right) dy \right. \\
 &+ m \int_{b_1}^{(b_1+b_2)} \left( \frac{h^2}{2} - \frac{x^2}{2\cos^2\gamma} + \frac{xy}{\sin\gamma} - \frac{y^2}{2}tg^2\gamma \right) dy \\
 &+ \left. \int_{(b_1+b_2)}^b \left( \frac{h^2}{2} - \frac{x^2}{2\cos^2\gamma} + \frac{xy}{\sin\gamma} - \frac{y^2}{2}tg^2\gamma \right) dy \right] \\
 &= R_{bt,ser1} \left\{ m \left[ \left( h^2 - \frac{x^2}{\cos^2\gamma} \right) \frac{b_2}{2} + \frac{xK_1\sin\gamma}{2\cos^2\gamma} - \frac{K_3}{6}tg^2\gamma \right] + \frac{(b_1+b_2)}{2} \right. \\
 &\cdot \left. \left( h^2 - \frac{x^2}{\cos^2\gamma} \right) + \frac{xK_2\sin\gamma}{2\cos^2\gamma} - \frac{K_4}{6}tg^2\gamma \right\} \\
 &= \frac{R_{bt,ser1}}{2} \left[ b_m \left( h^2 - \frac{x^2}{\cos^2\gamma} \right) + \frac{x\sin\gamma}{\cos^2\gamma} (mK_1 + K_2) \right. \\
 &\quad \left. - \frac{tg^2\gamma}{3} (mK_3 + K_4) \right].
 \end{aligned} \tag{10}$$

The coordinates of the center of gravity of the diagram of compressive and tensile stresses in concrete can be found by dividing the static moments of the compressed and tensile zones relative to the x and y axes by the value of the resultant compressive and tensile forces. Then the coordinates of the center of gravity of the compressive stress diagram relative to the y axis will be equal to:

$$x_b = \frac{\frac{x^3 b_n}{3 \cos \gamma} + \frac{x}{3} \sin \gamma (nK_3 + K_4) - \frac{x}{2} (nK_1 + K_2) - \frac{\sin^2 \gamma}{12} (nK_5 + K_6)}{2 \left[ \frac{x^2 b_n}{\sin \gamma} + \frac{\sin \gamma}{3} (nK_3 + K_4) - x(nK_1 + K_2) \right]} \quad (11)$$

The coordinates of the center of gravity of the compressive stress diagram relative to the x axis are determined by the following equation:

$$y_b = \frac{\frac{x^2 (nK_1 + K_2)}{4 \sin \gamma} - \frac{x}{3} (nK_3 + K_4) + \frac{\sin \gamma}{8} (nK_5 + K_6)}{\frac{x^2 b_n}{\sin \gamma} + \frac{\sin \gamma}{3} (nK_3 + K_4) - x(nK_1 + K_2)} \quad (12)$$

The coordinates of the center of gravity of the tensile stress diagram of the y axis is found from the expression:

$$y_{bt} = \frac{b_n \left( h^2 - \frac{x^2}{\cos^2 \gamma} \right) + \frac{x \sin \gamma}{\cos^2 \gamma} (mK_1 + K_2) - \frac{(mK_3 + K_4)}{3} t g^2 \gamma}{2 \left[ b_m \left( h - \frac{x}{\cos \gamma} \right) + \frac{mK_1 + K_2}{2} t g \gamma \right]} \quad (13)$$

The expression for determining the coordinate of the center of gravity of the tensile stress diagram relative to the x axis has the form:

$$y_{bt} = \frac{\frac{(mK_1 + K_2)}{2} \left( h - \frac{x}{\cos \gamma} \right) + \frac{(mK_3 + K_4)}{3} t g \gamma}{2 \left[ b_m \left( h - \frac{x}{\cos \gamma} \right) + \frac{mK_3 + K_4}{2} t g \gamma \right]} \quad (14)$$

The deformation in the i-th reinforcement bar is equal to (Fig. 2.1):

$$\varepsilon_{si} = \varepsilon_{bt} \frac{C_i - x}{H - x}. \quad (15)$$

Considering that

$$\begin{aligned} \varepsilon_{bt} &= \frac{2R_{bt,ser1}}{E_b}; \\ H &= b \sin \gamma + h \cos \gamma; \\ C_i &= x_{si} \cos \gamma + y_{si} \sin \gamma, \end{aligned}$$

after substitution into (2.15) we get:

$$\varepsilon_{si} = \frac{2R_{bt,ser1}}{E_b} \cdot \frac{x_{si} \cos \gamma + y_{si} \sin \gamma - x}{b \sin \gamma + h \cos \gamma - x} \quad (16)$$

The force in the i-th reinforcement bar is equal to:

$$N_{si} = 2R_{bt,ser1} \alpha \sum_{i=1}^n A_{si} \frac{x_{si} \cos \gamma + y_{si} \sin \gamma - x}{b \sin \gamma + h \cos \gamma - x}. \quad (17)$$

Results and discussion

To determine the height of the compressed zone of concrete, a condition is formulated for the sum of the projections of all acting forces on the longitudinal axis of the element to be equal to zero:

$$N_{bt} + \sum_{i=1}^n N_{si} = N_b + N, \quad (18)$$

or in expanded form:

$$2R_{bt,ser1} \left[ \left( h - \frac{x}{\cos \gamma} \right) b_m + \frac{tg \gamma}{2} (mK_1 + K_2) \right] + 2R_{bt,ser1} \alpha \sum_{i=1}^n A_{si} \frac{x_{si} \cos \gamma + y_{si} \sin \gamma - x}{b \sin \gamma + h \cos \gamma - x} \quad (19)$$

$$= \frac{R_{bt,ser1} \sin \gamma}{b \sin \gamma + h \cos \gamma - x} \left[ \frac{tg \gamma}{3} (nK_3 + K_4) + \frac{x^2 b_n}{\sin \gamma \cos \gamma} - \frac{x}{\cos \gamma} \cdot (nK_1 + K_2) \right]$$

Solving equation (2.19) for x, we obtain an expression for determining the height of the compressed zone of concrete:

$$x = \frac{(b \sin \gamma + h \cos \gamma) \left[ h b_m + \frac{tg \gamma}{2} (mK_1 + K_2) - \frac{N}{R_{bt,ser1}} \right] - (nK_3 + K_4) \frac{tg^2 \gamma}{3} + 2\alpha \sum_{i=1}^n A_{si} (x_{si} \cos \gamma + y_{si} \sin \gamma)}{b_m (2h + btg \gamma) + 2\alpha \sum_{i=1}^n A_{si} - \frac{N}{R_{bt,ser1}} + \frac{tg \gamma}{2} (mK_1 + K_2) - \frac{tg^2 \gamma}{3} (mK_1 + K_2)} \quad (20)$$

where  $\alpha$  – the ratio of the modulus of elasticity of the reinforcement to the initial modulus of elasticity of the concrete of the outer layers;

N – longitudinal force due to concrete shrinkage;

n – number of reinforcement bars in the section of the element.

With a compressed zone of concrete in the shape of a rectangle (case 1,8) and a trapezoid (case 5,7), the height of the compressed zone is determined by solving the quadratic equation. To determine the height of the compressed zone for a triangular shape (case 3), it is necessary to solve the cubic equation.

The implementation of the developed calculation algorithm in practice when designing wall panels, which experience horizontal and vertical force loads during the operational stage, is focused on the use of modern software systems that significantly reduce the engineer’s labor costs while making it possible to increase the accuracy of calculations by taking into account relatively small effective loads. In such cases, they were not taken into account or were taken into account by introducing safety factors.

Calculation of the formation of cracks in three-layer reinforced concrete elements during oblique bending with a multi-row arrangement of reinforcement along the cross-section is carried out based on the conditions:

$$M_x \leq M_{crc,x}; \quad M_y < M_{crc,y} \quad (21)$$

where  $M_{crc,x}$  и  $M_{crc,y}$  – moments perceived by a section normal to the longitudinal axis of the element when cracks form in the direction of the x and y axes.

$$M_{crc,x} = N_b (x_{bt} - x_b) + \sum_{i=1}^n N_{si} (x_{si} - x_{bt}) + N (x_{bt} - x_N); \quad (22)$$

$$M_{crc,y} = N_b (y_{bt} - y_b) + \sum_{i=1}^n N_{si} (y_{si} - y_{bt}) + N (y_{bt} - y_N),$$

where  $x_N$  and  $y_N$  are the coordinates of the point of application of the normal shrinkage force relative to the  $x$  and  $y$  coordinate axes. With  $N$  equal to the concrete shrinkage force  $P$ , the coordinates  $x_N$  and  $y_N$  will be equal:

$$x_N = \frac{\sum_{i=1}^n \sigma_{si} A_{si} x_{si}}{P}; \quad (23)$$

$$y_N = \frac{\sum_{i=1}^n \sigma_{si} A_{si} y_{si}}{P}; \quad (24)$$

where  $\sigma_{si}$  is the stress in the  $i$ -th reinforcement bar caused by concrete shrinkage.

Calculation of crack formation is performed using the MATLAB software package. The program for calculating the formation of cracks in three-layer reinforced concrete elements covers all practically possible positions of the neutral line in the section when the angles of inclination of the plane of the resultant external forces to the vertical change from  $0^\circ$  to  $90^\circ$  with a given number of reinforcement bars located arbitrarily.

The calculation is considered complete if the condition of parallelism of the plane of action of the moments of external and internal forces is satisfied. This condition can be achieved by performing a large number of computer cycles of calculation while gradually changing the angle of inclination of the neutral line to the horizontal. Initially, the angle of inclination is determined from elastic calculation. After determining the internal moments  $M_{cr,x}$  and  $M_{cr,y}$ , perceived by the normal section during the formation of cracks in the direction of the coordinate axes  $x$  and  $y$ , the tangent of the angle of inclination of the plane of action of the internal pair of forces to the vertical  $tg\beta^{int}$  is calculated. If, as a result of comparison, the tangent of the angle of inclination of the force plane  $tg\beta^{ext}$  is greater than the tangent of the angle of inclination of the plane of action of the internal pair of forces  $tg\beta^{int}$ , then the tangent of the angle of inclination of the neutral line  $tg\gamma$  increases by a given step size (0.001). If  $tg\beta^{ext}$  is less than  $tg\beta^{int}$ , then the tangent of the angle of inclination of the neutral line decreases by the same step. The calculation cycle ends if the difference between  $tg\beta^{ext}$  and  $tg\beta^{int}$ , reaches the specified minimum (0.01).

In the calculation program, additionally entered operators direct the machine to further solve the problem depending on the height of the compressed zone, determined as for an elastic body. The case is selected using boundary conditions:

$$\frac{x_{el}}{\sin\gamma} > b; \quad \frac{x_{el}}{\cos\gamma} > h,$$

where  $x_{el}$  – height of the compressed zone of concrete, determined from elastic calculation:

$$a = \frac{x_{el}}{\sin\gamma} - hctg\gamma.$$

If the condition is satisfied, the machine provides for determining the resultant forces in concrete and reinforcement, the coordinates of the points of application of the resultant forces in the compressed and tensile zones of concrete relative to the  $x$  and  $y$  axes, and the moments of cracking in the direction of the  $x$  and  $y$  axes.

The initial calculation data in the software package are:

$b, h$  – geometric parameters of the section, cm;

$b_1; b_3$  – thickness of outer layers, cm;

$b_2$  – thickness of the middle layer, cm;

$R_{bt,ser1}, R_{bt,ser2}$  – tensile strength of concrete of the outer layers and the middle heat-insulating layer, MPa;

$E_s$  – modulus of elasticity of reinforcing steel, MPa;

$E_{b1}, E_{b2}$  – initial elastic moduli of concrete of the outer layers and middle layer, MPa;  
 $A_s$  – cross-sectional area of working reinforcement, cm<sup>2</sup>;  
 $N$  – longitudinal force due to concrete shrinkage, MPa;  
 $tg\beta$  – tangent of the angle of inclination of the plane of action of the bending moment external forces to the vertical;  
 $n$  – number of rods in the element's section, pcs;  
 $0,0001$  – step size that decreases or increases  $tg\beta$ ;  
 $m$  – specified calculation accuracy.  
 The software package has been published:  
 $x_{el}$  – height of the compressed zone of concrete, determined from elastic calculation, cm;  
 $x$  – height of the compressed zone of concrete, found from the calculation of the formation cracks, cm;  
 $\gamma_{el}$  – angle of inclination of the neutral line to the horizontal from the elastic calculation, series;  
 $\gamma_{crc}$  – angle of inclination of the neutral line based on formation cracks, row;  
 $I_{red}^v$  – moment of inertia of the section relative to the x-axis;  
 $I_{red}^h$  – moment of inertia of the section relative to the y-axis;  
 $M_t$  – torque generated by eccentric application load, kN·m;  
 $N_s$  – forces arising in reinforcement bars, kN;  
 $N_b, N_{bt}$  – resultant forces in compressed and stretched zones concrete, MPa;  
 $x_b, x_{bt}$  – coordinates of the point of application of the resultant force in compressed and stretched zones of the section relative to the y-axis, cm;  
 $y_b, y_{bt}$  – coordinates of the point of application of the resultant force in compressed and stretched zones of the section relative to the x axis, cm;  
 $M_{crc,x}, M_{crc,y}$  – moments of crack formation in the direction x and y axes, kN·m.

The calculation for the formation of cracks using the proposed formulas was performed in the MATLAB software package for reinforced concrete beams of solid rectangular and three-layer sections. The beams are designed from heavy concrete with a strength of 1 MPa and reinforced at the section corners with class A3 (A400) rods with a diameter of 10 mm.

The angles of inclination of the force plane to the vertical are assumed to be equal 0°, 15°, 30°, 45°, 60°, 75°.

When the angles of inclination of the force plane to the vertical change from 0° to 75°, the values of the moments during the formation of cracks smoothly change from the largest to the smallest values corresponding to the values of the moments during the formation of cracks during plane bending.

The results of calculating the vertical and horizontal moments of cracking for beam samples at various angles of inclination of horizontal and vertical forces are given in Tables 1-8 depending on the thickness of the middle layer.

**Table 1.** Thickness of the middle layer  $b_2 = 0$  cm.

Angles	Material characteristics					Moments of crack- ing		MH / MV
	$R_{bt,1}$ , MPa / $b_1$ , cm	$R_{bt,2}$ , MPa / $b_2$ , cm	$R_{bt,3}$ , MPa / $b_3$ , cm	Diameter, mm	Fitting class	MH, kN·m	MV, kN·m	
0°	1,5 / 12,5	0,25 / 0	1,5 / 12,5	4Ø10	A500	0	3,5	0
15°	1,5 / 12,5	0,25 / 0	1,5 / 12,5	4Ø10	A500	1,01	3,15	0,32
30°	1,5 / 12,5	0,25 / 0	1,5 / 12,5	4Ø10	A500	1,6	2,4	0,67
45°	1,5 / 12,5	0,25 / 0	1,5 / 12,5	4Ø10	A500	1,9	1,87	1,02
60°	1,5 / 12,5	0,25 / 0	1,5 / 12,5	4Ø10	A500	2,1	1,3	1,62
75°	1,5 / 12,5	0,25 / 0	1,5 / 12,5	4Ø10	A500	2,28	0,8	2,85

**Table 2.** Thickness of the middle layer  $b_2 = 5$  cm.

Angles	Material characteristics					Moments of crack- ing		MH / MV
	$R_{bt,1}$ , MPa / $b_1$ , cm	$R_{bt,2}$ , MPa / $b_2$ , cm	$R_{bt,3}$ , MPa / $b_3$ , cm	Diameter, mm	Fitting class	MH, kN·m	MV, kN·m	
0°	1,5 / 10	0,25 / 5	1,5 / 10	4Ø10	A500	0	3,1	0
15°	1,5 / 10	0,25 / 5	1,5 / 10	4Ø10	A500	0,9	2,7	0,33
30°	1,5 / 10	0,25 / 5	1,5 / 10	4Ø10	A500	1,4	2,15	0,65
45°	1,5 / 10	0,25 / 5	1,5 / 10	4Ø10	A500	1,75	1,7	1,03
60°	1,5 / 10	0,25 / 5	1,5 / 10	4Ø10	A500	2	1,22	1,64
75°	1,5 / 10	0,25 / 5	1,5 / 10	4Ø10	A500	2,21	0,8	2,76

**Table 3.** Thickness of the middle layer  $b_2 = 7$  cm.

Angles	Material characteristics					Moments of crack- ing		MH / MV
	$R_{bt,1}$ , MPa / $b_1$ , cm	$R_{bt,2}$ , MPa / $b_2$ , cm	$R_{bt,3}$ , MPa / $b_3$ , cm	Diameter, mm	Fitting class	MH, kN·m	MV, kN·m	
0°	1,5 / 9	0,25 / 7	1,5 / 9	4Ø10	A500	0	2,7	0
15°	1,5 / 9	0,25 / 7	1,5 / 9	4Ø10	A500	0,75	2,3	0,33
30°	1,5 / 9	0,25 / 7	1,5 / 9	4Ø10	A500	1,25	1,9	0,66
45°	1,5 / 9	0,25 / 7	1,5 / 9	4Ø10	A500	1,6	1,58	1,01
60°	1,5 / 9	0,25 / 7	1,5 / 9	4Ø10	A500	1,9	1,12	1,70
75°	1,5 / 9	0,25 / 7	1,5 / 9	4Ø10	A500	2,12	0,75	2,83

**Table 4.** Thickness of the middle layer  $b_2 = 9$  cm.

Angles	Material characteristics					Moments of cracking		MH / MV
	$R_{bt,1}$ , MPa / $b_1$ , cm	$R_{bt,2}$ , MPa / $b_2$ , cm	$R_{bt,3}$ , MPa / $b_3$ , cm	Diameter, mm	Fitting class	MH, kN·m	MV, kN·m	
0°	1,5 / 8	0,25 / 9	1,5 / 8	4Ø10	A500	0	2,5	0
15°	1,5 / 8	0,25 / 9	1,5 / 8	4Ø10	A500	0,71	2,18	0,33
30°	1,5 / 8	0,25 / 9	1,5 / 8	4Ø10	A500	1,2	1,8	0,67
45°	1,5 / 8	0,25 / 9	1,5 / 8	4Ø10	A500	1,51	1,5	1,01
60°	1,5 / 8	0,25 / 9	1,5 / 8	4Ø10	A500	1,8	1,12	1,61
75°	1,5 / 8	0,25 / 9	1,5 / 8	4Ø10	A500	2,08	0,72	2,89

**Table 5.** Thickness of the middle layer  $b_2 = 11$  cm.

Angles	Material characteristics					Moments of crack- ing		MH / MV
	$R_{bt,1}$ , MPa / $b_1$ , cm	$R_{bt,2}$ , MPa / $b_2$ , cm	$R_{bt,3}$ , MPa / $b_3$ , cm	Diameter, mm	Fitting class	MH, kN·m	MV, kN·m	
0°	1,5 / 7	0,25 / 11	1,5 / 7	4Ø10	A500	0	2,3	0
15°	1,5 / 7	0,25 / 11	1,5 / 7	4Ø10	A500	0,65	2	0,33
30°	1,5 / 7	0,25 / 11	1,5 / 7	4Ø10	A500	1,1	1,7	0,65
45°	1,5 / 7	0,25 / 11	1,5 / 7	4Ø10	A500	1,42	1,4	1,01
60°	1,5 / 7	0,25 / 11	1,5 / 7	4Ø10	A500	1,75	1,05	1,67
75°	1,5 / 7	0,25 / 11	1,5 / 7	4Ø10	A500	2,02	0,7	2,89

**Table 6.** Thickness of the middle layer  $b_2 = 13$  cm.

Angles	Material characteristics					Moments of crack- ing		MH / MV
	$R_{bt,1}$ , MPa / $b_1$ , cm	$R_{bt,2}$ , MPa / $b_2$ , cm	$R_{bt,3}$ , MPa / $b_3$ , cm	Diameter, mm	Fitting class	MH, kN·m	MV, kN·m	
0°	1,5 / 6	0,25 / 13	1,5 / 6	4Ø10	A500	0	2,1	0
15°	1,5 / 6	0,25 / 13	1,5 / 6	4Ø10	A500	0,6	1,85	0,32
30°	1,5 / 6	0,25 / 13	1,5 / 6	4Ø10	A500	1,05	1,6	0,66
45°	1,5 / 6	0,25 / 13	1,5 / 6	4Ø10	A500	1,4	1,35	1,04
60°	1,5 / 6	0,25 / 13	1,5 / 6	4Ø10	A500	1,7	1,05	1,62
75°	1,5 / 6	0,25 / 13	1,5 / 6	4Ø10	A500	1,9	0,68	2,79

**Table 7.** Thickness of the middle layer  $b_2 = 15$  cm.

Angles	Material characteristics					Moments of crack- ing		
	$R_{bt,1}$ , MPa / $b_1$ , cm	$R_{bt,2}$ , MPa / $b_2$ , cm	$R_{bt,3}$ , MPa / $b_3$ , cm	Diameter, mm	Fitting class	MH, kN·m	MV, kN·m	MH / MV
0°	1,5 / 5	0,25 / 15	1,5 / 5	4Ø10	A500	0	1,9	0
15°	1,5 / 5	0,25 / 15	1,5 / 5	4Ø10	A500	0,55	1,72	0,32
30°	1,5 / 5	0,25 / 15	1,5 / 5	4Ø10	A500	1	1,52	0,66
45°	1,5 / 5	0,25 / 15	1,5 / 5	4Ø10	A500	1,35	1,3	1,04
60°	1,5 / 5	0,25 / 15	1,5 / 5	4Ø10	A500	1,68	1,02	1,65
75°	1,5 / 5	0,25 / 15	1,5 / 5	4Ø10	A500	1,9	0,68	2,79

**Table 8.** Thickness of the middle layer  $b_2 = 17$  cm.

Angles	Material characteristics					Moments of crack- ing		
	$R_{bt,1}$ , MPa / $b_1$ , cm	$R_{bt,2}$ , MPa / $b_2$ , cm	$R_{bt,3}$ , MPa / $b_3$ , cm	Diameter, mm	Fitting class	MH, kN·m	MV, kN·m	MH / MV
0°	1,5 / 4	0,25 / 17	1,5 / 4	4Ø10	A500	0	1,7	0
15°	1,5 / 4	0,25 / 17	1,5 / 4	4Ø10	A500	0,5	1,55	0,32
30°	1,5 / 4	0,25 / 17	1,5 / 4	4Ø10	A500	0,9	1,4	0,64
45°	1,5 / 4	0,25 / 17	1,5 / 4	4Ø10	A500	1,25	1,22	1,02
60°	1,5 / 4	0,25 / 17	1,5 / 4	4Ø10	A500	1,6	1	1,60
75°	1,5 / 4	0,25 / 17	1,5 / 4	4Ø10	A500	1,85	0,65	2,85

#### 4. CONCLUSIONS

In the practice of modern construction, three-layer enclosing structures are used, the layers of which consist of concrete with different physical and mechanical characteristics [17-20]. The strength and deformation characteristics of contact layers can influence the operation of a three-layer structure. To study the stress-strain state of such structures under the influence of loads, numerical methods are used, among other things. The studies were carried out on bendable three-layer structural models using a middle layer of various thicknesses made of low-strength concrete. The influence of geometric, strength and deformation characteristics of layers on the results of calculations of bendable three-layer structures has been established. Calculation models have been constructed and formulas for calculating bendable three-layer reinforced concrete structures have been derived, taking into account the influence of the geometric, strength and deformation characteristics of the middle layer. The obtained research results make it possible to determine rational parameters for the design of three-layer enclosing structures with reinforced concrete layers of different strengths connected to each other by a monolithic contact layer.

#### REFERENCES

- [1] Fernando P.L.N., Jayasinghe M.T.R., Jayasinghe C. Structural feasibility of Expanded Polystyrene (EPS) based lightweight concrete sandwich wall panels. Construction and Building Materials. 2017. 139. P. 45 – 51.
- [2] Koyankin A.A., Mitasov V.M., Deordiev S.V. The compatibility of deformation of the hollow-core slab with beams. Magazine of Civil Engineering. 2019. 3 (87). P. 93 – 102.

- [3] Diamond S. Aspects of concrete porosity revisited. *Cement and Concrete Research*. 1999. 29 (8). P. 1181 – 1188.
- [4] Shendy M.E. A comparative study of LECA concrete sandwich beams with and without core reinforcement. *Cement and Concrete, Compos.* 1991. 13. P. 143 – 149.
- [5] Korol E.A. The choice of the rational parameters of three-layer reinforced concrete enclosing structures with the monolithic bond of layers by computer simulation. *IOP Conference Series: Materials Science and Engineering*. 2018. 456. 7 p.
- [6] Shams A., Horstmann M., Hegger J. Experimental investigations on Textile-Reinforced Concrete (TRC) sandwich sections. *Composite Structures*. 2014. 118. P. 643 – 653.
- [7] Andreev V.I., Turusov R.A., Tsybin N.Y. Application of the Contact Layer in the Solution of the Problem of Bending the Multilayer Beam. *Procedia Engineering*. 2016. 153. P. 59 – 65.
- [8] Gara F., Ragni L., Roia D., Dezi L. Experimental behaviour and numerical analysis of floor sandwich panels. *Eng. Struct.* 2012. 36. P. 258 – 269.
- [9] Gara F., Ragni L., Roia D., Dezi L. Experimental tests and numerical modelling of wall sandwich panels. *Eng. Struct.* 2012. 37. P. 193 – 204.
- [10] Tho V.D., Korol E.A. Influence of geometrical parameters of the cross section, strength and deformability of the materials used on stress-strain state of three-layered reinforced concrete. *IOP Conference Series: Materials Science and Engineering*. 2019. 661. P. 10.
- [11] Yue Z., Xiao H. Generalized Kelvin Solution based boundary element method for crack problems in multilayered solids. *Engineering Analysis with Boundary Elements*. 2002. 26. P. 691 – 705.
- [12] Siddika A., Al Mamun M.A., Ferdous W., Alyousef R. (). Performances, challenges and opportunities in strengthening reinforced concrete structures by using FRPs—A state-of-the-art review. *Engineering Failure Analysis*. 2020. 111. P. 104480.
- [13] Marciukaitis G., Juknevičius L. Influence of the Internal Layer Cracks on the Cracking of Flexural Three-Layer Concrete Members. *Journal of Civil Engineering and Management*, 2002. 8. P. 153 – 158.
- [14] Tamrazyan A.G., Popov D.S., Ubysz A. To the dynamically loaded reinforced-concrete elements' calculation in the absence of adhesion between concrete and reinforcement. In *IOP Conference Series: Materials Science and Engineering*. 2020, August. Vol. 913. 2. P. 022012). IOP Publishing.
- [15] Funari M.F., Spade S., Fabbrocino F., Luciano R.A. Moving Interface Finite Element Formulation to Predict Dynamic Edge Debonding in FRP-Strengthened Concrete Beams in Service Conditions. *Fibers*. 2020. 8. 42 p.
- [16] Funari M.F., Greco F., Lonetti P. A cohesive finite element model based ALE formulation for z-pins reinforced multilayered composite beams. *Procedia Struct.Integr.* 2016. 2. P. 452459.
- [17] Moaveni S. *Finite element analysis: Theory and application with ANSYS*, 2015, (in London).
- [18] Howiacki T., Sieńko R., Bednarski Ł., Zuziak, K. Crack shape coefficient: comparison between different DFOS tools embedded for crack monitoring in concrete. *Sensors*. 2023. 23 (2). P. 566.
- [19] Shilov A.V., Beskopylny A.N., Meskhi B., Mailyan D., Shilov D., Polushkin O.O. (). Ultimate Compressive Strains and Reserves of Bearing Capacity of Short RC Columns with Basalt Fiber. *Applied Sciences*. 2021. 11 (16). P. 7634.
- [20] Belostotsky A., Pavlov A., Nagibovich A. Numerical simulation of the stress-strain state of a large-span structure with joints with gap under the seismic loads in a transient dynamic. *International Journal for Computational Civil and Structural Engineering*. 2023. 19 (3). P. 165 – 172.

## INFORMATION ABOUT THE AUTHORS

**Korol O.A.**, KorolOA@mgsu.ru, ORCID ID: 0000-0001-6887-014X, SCOPUS: <https://www.scopus.com/authid/detail.uri?authorId=57201189430>, National Research Moscow State University of Civil Engineering (NRU MGSU), Candidate of Technical Sciences, Professor, Associate Professor, Department of Housing and Communal Complex, 129337 Moscow Yaroslavskoe Highway 26

**Barabanova T.A.**, BarabanovaTA@mgsu.ru, ORCID ID: 0000-0002-1212-8744, SCOPUS: <https://www.scopus.com/authid/detail.uri?authorId=6603493660>, National Research Moscow State University of Civil Engineering (NRU MGSU), Candidate of Technical Sciences, Associate Professor, Associate Professor, Department of Housing and Communal Complex, 129337 Moscow Yaroslavskoe Highway 26

**Sabitov L.S.**, e-mail: l.sabitov@bk.ru, тел. 89377740700, ORCID ID: <https://orcid.org/0000-0001-7381-9752>, SCOPUS: <https://www.scopus.com/authid/detail.uri?authorId=57079229700>, Kazan (Volga Region) Federal University, Department of Structural and Design Engineering, Doctor of Engineering Sciences (Advanced Doctor), Professor

**Abdullazyanov E.U.**, e-mail: kgeu@kgeu.ru, тел. 843 5194202, ORCID ID: <https://orcid.org/0009-0007-7006-2265>, SCOPUS: <https://www.scopus.com/authid/detail.uri?authorId=56700289800>, Kazan State Energy University, Candidate of Technical Sciences, Rector

**Ayzatullin M.M.**, e-mail: marat.ayzatullin@tatar.ru, тел. 843 2311501, ORCID ID: <https://orcid.org/0009-0008-1813-4820>, Kazan State Energy University, Postgraduate